International Conference on Space Optics—ICSO 2018

Chania, Greece

9–12 October 2018

Edited by Zoran Sodnik, Nikos Karafolas, and Bruno Cugny

Q³Sat: quantum communications uplink to a 3U CubeSat: feasibility and design

Sebastian Neumann

Siddarth Joshi

Thomas Scheidl

Roland Blach

et al.

International Conference on Space Optics — ICSO 2018, edited by Zoran Sodnik, Nikos Karafolas, Bruno Cugny, Proc. of SPIE Vol. 11180, 111801V · © 2018 ESA and CNES · CCC code: 0277-786X/18/$18 · doi: 10.1117/12.2535986

Feasibility of a 3U CubeSat for Uplink Quantum Communications

Sebastian P. Neumann*[a,b‡], Siddarth K. Joshi[a,b‡], Thomas Scheidl[a,b], Roland Blach[a], Carsten Scharlemann[c], Sameh Abouagaga[c], Daanish Bambery[c], Erik Kerstel[d], Mathieu Barthelemy[d], Rupert Ursin[a,b], Matthias Fink[a]

[a]Institute for Quantum Optics and Quantum Information Vienna, Vienna, Austria; [b]Vienna Center for Quantum Science and Technology, Vienna, Austria; [c]University of Applied Sciences Wiener Neustadt, Wiener Neustadt, Austria; [d]Laboratoire Interdisciplinaire de Physique, University Grenoble Alpes, Saint-Martin-d'Hères, France

[‡]Equal Contributors

***DISCLAIMER**: Another version of this work has been published with SpringerOpen as an "open-access" peer-reviewed paper under a Creative Commons license. It can be accessed in its entirety on the EPJ Quantum Technology website[1].*

ABSTRACT

In the absence of technically mature quantum repeaters, losses in optical fibers limit the distance for ground-bound quantum key distribution (QKD). One way to overcome these losses is via optical links to satellites, which has most prominently been demonstrated in course of the Chinese-Austrian QUESS mission. Though its findings were impressive, such a large-scale project requires massive financial and time resources. We propose a 34x10x10cm³ nanosatellite orders of magnitude cheaper which is able to perform QKD in a trusted-node scenario, using only commercially available components.

We have performed a detailed analysis of such a CubeSat mission ("Q³Sat"), finding that cost and complexity can be reduced by sending the photons from ground to satellite, i.e. using an uplink. Calculations have been done for a prepare-and-send protocol (BB84 with decoy pulses) using polarization as information carrier. We have created a preliminary design of a 3U CubeSat including a detailed size, weight and power budget and a CAD to account for the assembly of the components. Deploying a 10 cm long mirror telescope covering the small surface of the satellite leaves enough space for a polarization analysis module and housekeeping, communication and computing electronics.

For one such CubeSat, we estimate the quantum secure key to be acquired between two ground stations during one year to be about 13 Mbit. A Bell test between ground and satellite would also be feasible. The uplink design allows to keep the more sensitive, computation-intensive and expensive devices on ground. The experiment proposed by us therefore poses a comparably low-threshold quantum space mission. For a two-year lifetime of the satellite, the price per kilobit would amount to about 20 Euro. In large constellations, Q³Sats could be used to establish a global quantum network, which would further lower the cost. Summarizing, our detailed design and feasibility study can be readily used as a template for global-scale quantum communication.

Keywords: Quantum communication, Optical uplink, CubeSat, Quantum Key Distribution, Feasibility study, Satellite technology, Atmospheric losses, Quantum optics

*sebastian.neumann@univie.ac.at; phone +43 1 4277 29560; iqoqi-vienna.at

1. INTRODUCTION

The security of quantum communication (Q.Com) is based on fundamental and immutable laws of physics and not on the assumption that a problem is and always will be too difficult for an adversary to solve. Naturally, this unconditionally secure communication technology has a large impact on global communications. Attempts to overcome the limits imposed by losses, such as Ref. [2], and attempts to create a global satellite based network, are underway[3,4]. The latter are large and complex satellites which can cost upwards of 100 M€ each. Small CubeSats however can be constructed and launched for 0.5 to 10 M€.We present a simple, small, light-weight and low power-consuming satellite system capable of Q.Com. Our CubeSat mission is called Q³Sat (pronounced Q-CubeSat). Previous long distance implementations via optical fiber such as Ref. [5] and free space terrestrial links like Ref. [6] have approached the limits of terrestrial Q.com in terms of distance. The successful 600 kg class[3] and 50 kg class[7] large satellites have shown that Q.com in space is feasible. By analyzing the results of these proof-of-concept missions and evaluating their performance in both the uplink and the downlink scenario, we find that a downlink scenario offers a larger key rate. In an uplink, only a relatively simple polarization analysis module needs to be on board the satellite and a ultra bright state-of-the-art quantum source can be used on ground. Thus, an uplink is more suitable for a low cost CubeSat mission. Additionally, an uplink allows for a larger variety of implementable Q.Com protocols. This is because many different Q.Com protocols (e.g., E91[8], BB84[9], decoy state protocol (DSP)[10], BBM[11], B92[12]) rely on nearly identical detection schemes for the receiver and can thus all be implemented on our CubeSat. Changes would only have to be made to the easily accessible ground module. The CubeSat design considered here will also be able to perform tasks beyond Q.Com, e.g. measuring light pollution stemming from ground with a narrow field of view (FoV) to establish a global map in unprecedented resolution at single-photon level. This is crucial to finding dark areas near potential Q.Com customers and for other, more general applications. Additionally, the timing resolution of the single photon detectors enables pulse position modulation in classical communication from ground to space with exceptionally fast data rates. The extremely sensitive single photon detectors can also be re-purposed for other terrestrial and astronomical observations requiring an exceptional cadence and narrow FoV. In this manuscript we nevertheless focus on Q.Com, since this objective drives the design for the satellite infrastructure.

2. CUBESAT DESIGN

The advantage of the uplink scenario is that most of the mission's complexity is ground-based. Figure 1 shows an overview of the experiment consisting of space and ground segments.

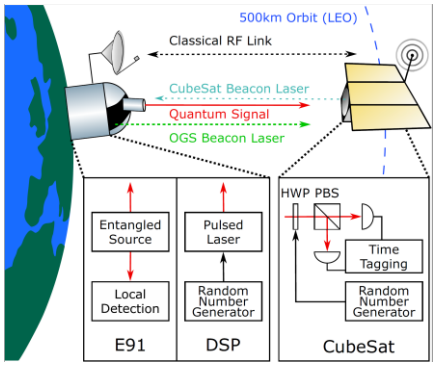

Figure 1. The optical ground station (OGS) is connected either to one arm of a source of polarization entangled photon pairs (E91, not considered in this paper) or to a pulsed laser with randomly chosen polarization and mean photon number for each pulse (DSP). The signal photons are transmitted to the CubeSat in a 500 km low-earth orbit (LEO) via a free-space link. OGS and CubeSat point beacon lasers at each other for precise attitude control. The quantum signal is analyzed on board the CubeSat using a randomly switched half-wave plate (HWP) and a polarizing beam splitter (PBS). Measurement outcome, basis choice and time tag of each event are recorded. Information about the latter two is transmitted to the OGS using a classical radio frequency (RF) link. The OGS identifies the matching bits using a cross-

correlation analysis and tells the CubeSat which ones to use. Both disregard the other bits, perform post-processing and then share a secret key.

The CubeSat requires several subsystems as shown in the CAD-design (Fig. 2). For a 3U CubeSat, its components must be arranged to fit within a total volume of $0.1 \times 0.1 \times 0.32$ m^3, have a combined mass of less than 4 kg and consume a maximum of 21 Wh per orbit (with deployable $\approx 30 \times 30$ cm^2 off-the-shelf solar panels[13]).

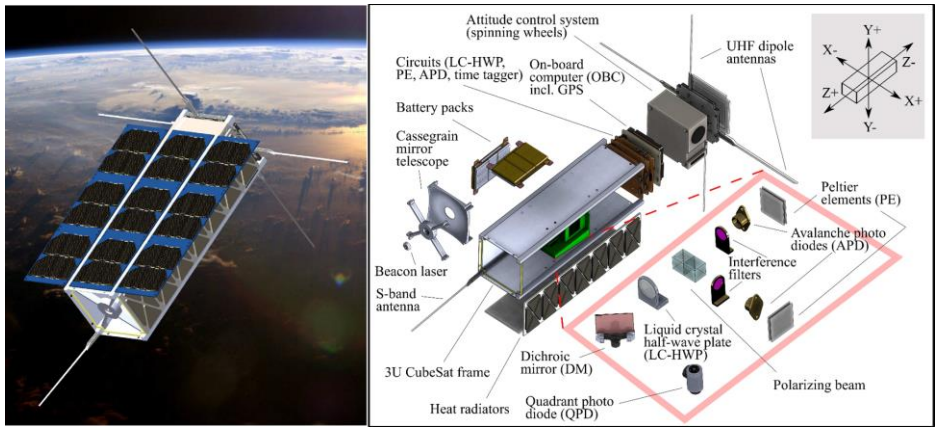

Figure 2. *Left*: Artistic depiction of the 3U CubeSat with deployable solar panels in bird-wing configuration. They are mounted to the sun-facing side of the CubeSat, the other three long sides of the surface can be covered with radiators for detector cooling. *Right:* Exploded view of our preliminary 3U CubeSat design. The solar panels as well as any electric connections have been omitted for clarity. The optical elements shown in the red box are out of scale.

In this section we focus on the quantum payload which consists of receiving telescope, basis choice, polarization analysis and detection subsystems (see Fig. 3).We estimate all optical losses within the CubeSat (between telescope and detectors) to be 1.0 dB, using only standard commercially available devices[14-16]. The most crucial performance parameters are the noise counts of the avalanche photo diodes (APDs), which we will discuss in more detail in the following sections.

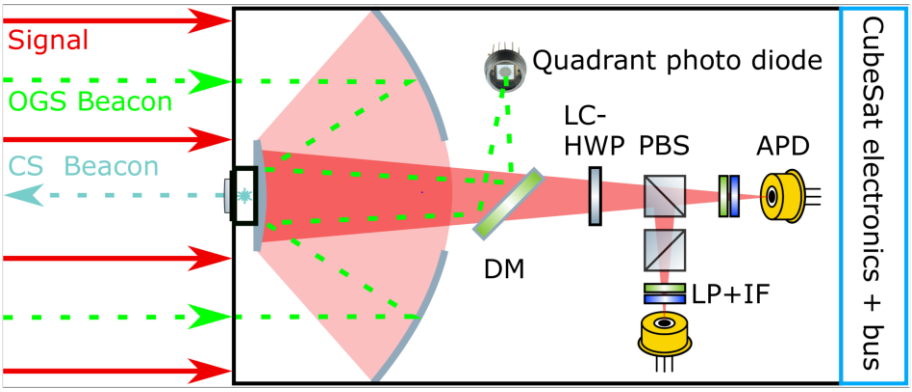

Figure 3. Schematic of the optics payload on board the 3U CubeSat. The signal and beacon beams from ground are collected by a Cassegrain-type mirror telescope. The back side of the secondary mirror carries the earth-facing beacon laser necessary for tracking of the CubeSat. The input signal and beacon are separated by a dichroic mirror (DM). The latter is tracked with a fast quadrant detector for precise attitude sensing and clock synchronization while the former passes a binary liquid-crystal-based half-wave plate switch (LC-HWP). It randomly shifts the polarization of incoming photons by either 0 or $\pi 4$. This effectively acts as a measurement basis switch in combination with the polarizing beam

splitter (PBS) separating horizontally (vertically) polarized photons by transmitting (reflecting) them. The second PBS is used for enhanced extinction ratios. Longpass (LP) and interference filters (IF) are used to block out stray light and the photons are detected by silicon-based avalanche photo diodes (APD).

2.1 Limiting noise counts

The most challenging aspect of designing a CubeSat is minimizing total noise counts R_{B+D} which therefore influences many design parameters. Unavoidable stray light collected by the CubeSat's receiving telescope (i.e., background counts R_{BG}) and the intrinsic thermal/ radiation damage counts of the detectors (i.e., dark counts per detector R_{DC}) add up to $R_{B+D} = R_{BG} + 2R_{DC}$ and significantly degrade the signal-to-noise ratio (SNR). R_{DC}, which we assume to be constant, has to be below 200 cps per detector to achieve a reasonable SNR. Firstly, the detector noise is reduced when operating at low temperatures. –30°C diode temperature is desirable. Two 250 cm^2 radiators on the sun-averted sides of the CubeSat could dissipate the 0.6 W of thermal energy required to cool both detectors. A heating resistor should be used to further regulate the temperature to within ±1°C. While R_{DC} of such a cooled detector can be less than 5 cps in laboratory conditions[17], it is increased by damage due to energetic particles and ionizing radiation in space. This can be mitigated by using very small active detector areas d_B. The smallest commercially available ones have a d_B of 20 µm, which we expect to be small enough to keep R_{DC} well below the 200 cps limit[18] despite a radiation damage equivalent to a 2 year mission lifetime. Using other satellite components such as high density batteries accounts for additional radiation shielding. We therefore assume a constant 200 cps of thermal and radiation noise per detector which is, at least for the first months of operation, a conservative estimate.

R_{BG} are the erroneous measurement clicks due to near-infrared noise photons originating from the ground area which are not blocked by the spectral filters. As a worst-case scenario, we account for scattered sunlight from a full moon (brightness: 4000 cd/m²)[19] reflected from earth (mean albedo: 0.3)[20] into to the CubeSat (we used the solar radiation spectrum). We then translate the luminous intensity into photons per second per m^2 footprint impinging on the CubeSat telescope with aperture D_B = 10 cm and calculate how many of these photons would pass through our 3 nm wide bandpass filters centered at 810 nm. We arrive at values of 0.55 photons $s^{-1}m^{-2}$ in zenith and 0.17 photons $s^{-1}m^{-2}$ for the lowest elevations (because of the larger distance between OGS and satellite). This effect of decreasing background counts per area for low elevations is however less significant than the increase in area because of the larger footprint on ground. The closer the CubeSat is to the horizon, the more ground area is covered by the satellite's FoV since the circular footprint in zenith changes to a substantially larger elliptical one. Optical losses and detection efficiency of the CubeSat on the other hand reduce the background count value again (see below in this section). In total this gives us a worst-case estimate of total noise counts which we use for all orbits regardless of the moon phase: R_{B+D} varies from ≈480 cps in zenith to ≈575 cps at 30° elevation from horizon. This assumption is very conservative, especially when considering the 350 cps total noise counts at full moon of a similar uplink experiment[21].

2.2 Field of View (FoV) and attitude control

For a given orbit height of 500 km and imperfect filters, R_{BG} can only be reduced by reducing the field of view (FoV = d_B/f_B where f_B is the CubeSat telescope's effective focal length). This has two additional benefits: A long f_B improves the polarizing beam splitter's (PBS) extinction ratio since it reduces the divergence of the impinging beam within the PBS. More importantly, a small d_B strongly reduces the radiation damage to the detector due to its small cross sectional area. However, the FoV must be large enough to maintain the OGS in view despite the pointing errors of the CubeSat. Until recently, the attitude control of small CubeSats was too imprecise, requiring a large FoV that would have resulted in too many background counts to make the mission possible. The latest commercially available CubeSat attitude control systems based on star trackers have shown a body pointing precision σ_B of better than 40 µrad RMS (full angle)[22,23]. The resulting pointing losses Λ_{PB} due to this error, which are caused by an effective spot size broadening on the detectors when averaging over time, can be shown to be

$$\Lambda_{PB} = 1 - \exp\left[-\frac{\frac{1}{2}FoV^2}{\left(\frac{2\lambda}{\pi D_B}\right)^2 + \sigma_B^2}\right]$$

This attitude precision allows us to limit the FoV < 50 µrad while introducing pointing losses $1/\Lambda_{PB}$ of 2.5 dB. These comparably high losses are outbalanced by the strongly reduced R_{BG} because of the narrow FoV. Roll axis precision is

about a factor of 10 worse[24], however misalignment here only leads to an increase in erroneous detections e_d on the CubeSat. Even with misalignment in the order of tens of mrad, its contribution to e_d stays below 0.1%. Optically tracking the beacon signal holds the potential to further improve Λ_{PB}. Another attitude system requirement is a sufficient slew rate. To keep the OGS in view, the CubeSat should be able to turn with up to 1°/s; this can easily be provided by the system in consideration (10°/s slew rate in pitch and yaw axes for a 4 kg 3U CubeSat[22]). To achieve an optimal f_B, a Cassegrain-type reflector is a good choice for the receiving telescope despite the decreased telescope transmission due to the secondary mirror (which we estimate to be –1.5 dB in total). This is because the overall design is lightweight and the required f_B of 40 cm can be realized with a 10 cm long telescope. The telescope covers the CubeSat's square Z+ surface of about 9 × 9 cm. For simplicity, our calculations assume a circular telescope with D_B = 10 cm.

2.3 Dead time and timing resolution

To ensure that saturation and dead time effects do not cause losses >0.1 dB, we require a maximum count rate of each CubeSat detector in the order of 100 kHz. The detectors consist of actively quenched silicon-based avalanche photo diodes (APDs) operated in Geiger mode, placed at the output ports of the PBS. The detector diameter d_B of only 20 µm strongly reduces the cross sectional area for harmful radiation. Therefore little to no radiation shielding is required, which also has a positive effect on the mass budget.
Errors in Q.Com arise from accidental coincidences and are therefore related to the coincidence detection time window τ. To correctly identify and distinguish at least 98% of all pairs, τ has to be greater than $\approx 2\sqrt{(t_A^2 + t_B^2)}$, where t_A = 10 ps is the timing jitter on ground and t_B that on the CubeSat. Thus t_B, including the jitter of the detectors[17] and the time tagging electronics that note the arrival time of each pulse[25,26], should be less than 40 ps to ensure that we can choose τ = 80 ps which is crucial to improving the SNR. The detection efficiency of the detectors η_B we chose is ≈15%. This might seem low, however we trade this for excellent temporal resolution.
In addition to the quantum payload, the CubeSat optics should also accommodate an earth-facing beacon diode to aid in the ground station's tracking of the CubeSat. There should also be a dichroic mirror to separate the quantum signal from the OGS beacon. The latter assists in locating and tracking the OGS and can be detected by a fast quadrant photo diode. The OGS's beacon signal is pulsed to facilitate clock synchronization, and the detection pulses from the fast photo diode (along with GPS signals) are used to discipline the local clock on board the CubeSat.

3. PERFORMANCE ANALYSIS

We now want to give an estimate on the amount of secret key the satellite could acquire with two sufficiently separated OGS over one year. To this end, we derive a model for geometric losses due to beam divergence while incorporating long-time measurements of atmospheric turbulence and weather influences to calculate different loss scenarios for our uplink. We also carry out an orbit assessment (see Fig. 5).

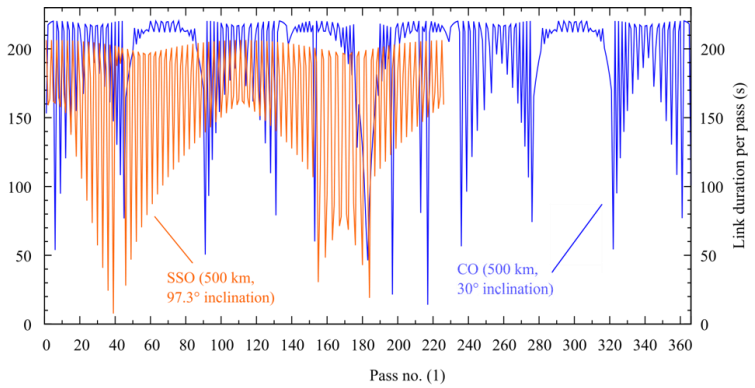

Figure 5: 500 km LEO orbits that appear with more than 30° elevation from horizon and are visible between 0:00 and 6:00am over La Palma for different inclinations. Comparison of the link duration between two 500 km low-earth orbits (LEOs): 97.3° sun-synchronous (red) and the optimal 30° circular orbit (blue). Only passes with more than 30° maximum

elevation at night are shown. The average visible time per pass is 195 s (163 s) for CO (SSO), the total visible time per year amounts to 71,435 s (37,115 s) for CO (SSO).

Lastly, we evaluate the requirements for an on board clock and estimate the data storage and -transmission needs as well as the computational requirements of the CubeSat. Measurements by the RoboDIMM seeing monitor on La Palma show that a Fried parameter r_0 of larger than 5 cm can on average be observed on 228 nights per year (see Fig. 6) or 62% of the time. Therefore, assuming a circular orbit with 30° orbital inclination, it can be assumed that for a total of 44,300 s or 12:20 h each year, the link quality is sufficient to perform Q.Com. The average inclination in zenith as seen from the OGS is 28.3° (unlike the orbital pass shown in Fig. 6 where the zenith angle goes down to 0°). Computing for such an average orbit and taking the annual r_0 values into account, the total key acquired in one year would therefore amount to 13.0Mbit for a DSP protocol.

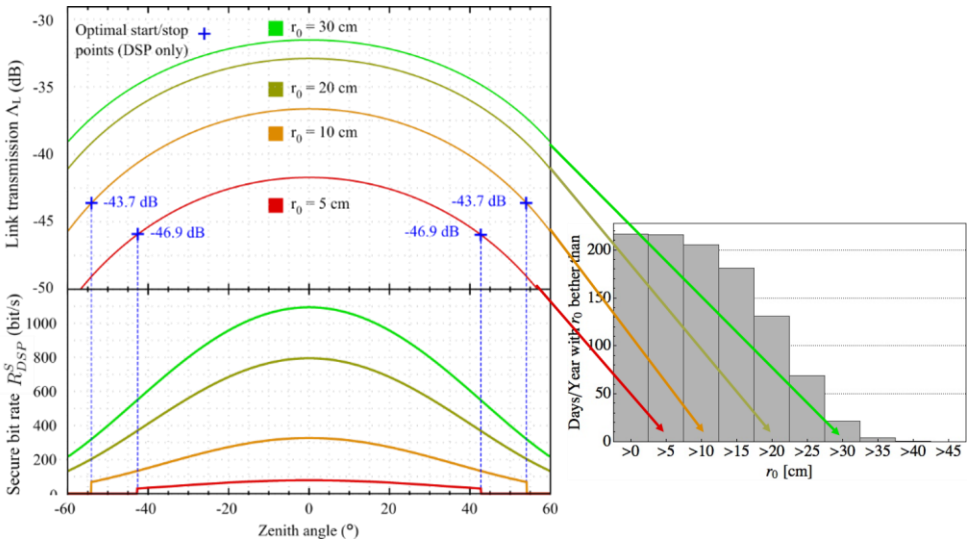

Figure 62 Link Loss Λ_L and secure key rates R^S_{DSP} as functions of zenith angle ϕ. All curves are shown for 0° incliniation w.r.t. the OGS. Similar curves can be calculated for different inclination angles. *Top left:* Link transmission $\Lambda_L(\phi)$ of a 500 km orbit for different Fried parameters r_0. A minimum elevation from horizon of 30° is required (i.e. $|\phi| \leq 60°$). *Bottom left:* Secure key rates for DSP using optimal starting points for those values of r_0 that are too small to allow communication throughout the orbit (marked by pluses). The temporal integral over these curves, i.e. the total key acquired during one pass, amounts to 6.8 kbit (r_0 = 5 cm), 33.9 kbit (10 cm), 95.2 kbit (20 cm) and 137.4 kbit (30 cm) respectively. *Right*: Histogram of days per year with certain Fried parameters r_0, averaged over nine years starting in February 2008. Insufficient weather conditions (clouds, rain, winds) as well as technical problems lead to N = 228 instead of 365. The average daily r_0 is 19.7 cm.

4. CONCLUSION

Using our CubeSat design, a pair of ground stations can exchange $13x10^6$ secure bits a year (ignoring finite key effects). Our CubeSat design consists of commercially available components that cost <200,000€[27]. A typical launch price is <300,000€[28].Naturally, the research/development and manpower costs for the first such satellite would be higher and are not included. Assuming a lifetime of two years, information theoretic security could be bought for ≈20€/kbit, provided that an operational OGS is readily available. For DSP, such an OGS would be about 100,000€.

In the current design, the CubeSat is a trusted node. This is suitable for usage scenarios like communication between many branches of a single organization. The current state-of-the-art Q.com satellites are prohibitively expensive trusted nodes, for communication across the globe, that can only be built by a few select industries. A CubeSat – such as we have shown above – is cheaper and interested organizations can build their own or carefully supervise the building of these trusted nodes for their own use. The proposed CubeSat can also be used for fundamental experiments such as Bell tests which require a SNR of only 4.8 (as opposed to the SNR of 15.1 needed by DSP QKD), clock synchronization, light pollution measurements and earth/atmosphere observation at the beacon wavelengths.

REFERENCES

[1] Neumann SP, Joshi SK, Fink M, Scheidl T, Blach R, Scharlemann C et al.: "Q³Sat: quantum communications uplink to a 3U CubeSat – feasibility & design", EPJ Quantum Technology, 5, 4 (2018)
[2] Azuma K, Mizutani A, Lo HK: "Fundamental rate-loss trade-off for the quantum Internet". Nat Commun. 2016;7:13523.
[3] Yin J, Cao Y, Li YH, Liao SK, Zhang L, Ren JG, et al. "Satellite-based entanglement distribution over 1200 kilometers", Science. 2017;356(6343):1140–4.
[4] Liao SK, Cai WQ, Liu WY, Zhang L, Li Y, Ren JG, et al. "Satellite-to-ground quantum key distribution", Nature. 2017;549:43–7.
[5] Yin HL, Chen TY, Yu ZW, Liu H, You LX, Zhou YH, et al. "Measurement-device-independent quantum key distribution over a 404 km optical fiber", Phys Rev Lett. 2016;117(19):190501.
[6] Ursin R, Tiefenbacher F, Schmitt-Manderbach T, Weier H, Scheidl T, Lindenthal M, et al.: "Free-space distribution of entanglement and single photons over 144 km", Nat Phys. 2007;3:481–6.
[7] Takenaka H, Carrasco-Casado A, Fujiwara M, Kitamura M, Sasaki M, Toyoshima M: "Satellite-to-ground quantum-limited communication using a 50-kg-class microsatellite", Nat Photonics. 2017;11:502–8.
[8] Ekert AK.: "Quantum cryptography based on Bell's theorem", Phys Rev Lett. 1991;67(6):661.
[9] Bennett CH, Brassard G: "Quantum cryptography: public key distribution and coin tossing", In: Int. conf. on computers, systems and signal processing. Bangalore, India. Dec. 1984. 1984. p. 175–9.
[10] Lo HK, Ma X, Chen K: "Decoy state quantum key distribution", Phys Rev Lett. 2005;94:230504.
[11] Bennett CH, Brassard G, Mermin ND: "Quantum cryptography without Bell's theorem", Phys Rev Lett. 1992;68(5):557.
[12] Bennett CH: "Quantum cryptography using any two nonorthogonal states", Phys Rev Lett. 1992;68(21):3121.
[13] Brochure for deployable solar panels from cubesatshop.com. 2016. http://www.cubesatshop.com/wp-content/uploads/2016/07/EXA-DSA-Brochure-1.pdf. Accessed 2017-10-17.
[14] Aperture Optical Systems CubeSat telescope. 2017. http://www.apertureos.com/products/cube-sat. Accessed 2017-10-17.
[15] Thorlabs dielectric filters. 2017. https://www.thorlabs.com/navigation.cfm?guide_id=2210. Accessed 2017-10-17.
[16] Thorlabs polarizing beam splitters. 2017. https://www.thorlabs.de/newgrouppage9.cfm?objectgroup_id=739. Accessed 2017-10-17.
[17] MPD PDM series data sheet. 2017. http://www.micro-photon-devices.com/Docs/Datasheet/PDM.pdf. Accessed 2017-11-04.
[18] Anisimova E, Higgins BL, Bourgoin JP, Cranmer M, Choi E, Hudson D, et al: "Mitigating radiation damage of single photon detectors for space applications", EPJ Quantum Technol. 2017;4(1):10.
[19] "Luminance and brightness data for the full moon", 2009. http://spaceweather.com/swpod2009/13jan09/Perigee_moon_2009_01_11_corr.pdf. Accessed 2017-10-20.
[20] Stephens GL, O'Brien D, Webster PJ, Pilewski P, Kato S, Li J: "The albedo of Earth", Rev Geophys. 2015;53(1):141–63.
[21] Ren JG, Xu P, Yong HL, Zhang L, Liao SK, Yin J, et al.: "Ground-to-satellite quantum teleportation", Nature. 2017;549(7670):70–3.
[22] Blue Canyon XACT data sheet. 2017. http://bluecanyontech.com/wp-content/uploads/2017/07/DataSheet_ADCS_08_F.pdf. Accessed 2017-10-17.
[23] This value is expected for the Blue Canyon XB-1 spacecraft bus which is entirely compatible with our design. Personal communication with Josh Duncan. Blue Canyon Technologies. For the XB-1 bus specifications see. 2017. http://mstl.atl.calpoly.edu/~bklofas/Presentations/SummerWorkshop2012/Stafford_XB1.pdf. Accessed 2017-10-20.
[24] Mason JP, Baumgart M, Rogler B, Downs C, Williams M, Woods TN, et al.: "MinXSS-1 CubeSat on-orbit pointing and power performance: the first flight of the Blue Canyon technologies XACT 3-axis attitude determination and control system", 2017. arXiv:1706.06967.
[25] Picoquant TimeHarp 260 data sheet. 2017. https://www.picoquant.com/images/uploads/downloads/timeharp260.pdf. Accessed 2017-10-17.
[26] Personal communication with Dr. Michael Schlagmueller. Swabian Instruments. 2017.

[27] CubeSatShop one-stop webshop for CubeSats and Nanosats. 2018. https://www.cubesatshop.com/. Accessed 2018-02-15.
[28] Spaceflight launch company. 2017. http://spaceflight.com/schedule-pricing/#pricing. Accessed 2017-10-17.